



Probing the ‘Venus fly-trap’ parameters of cyclo-octadiene in selected β -diketonato complexes of platinum(II) and the nickel-triad from a spectroscopic, X-ray crystallographic and DFT study

T.N. Hill, A. Roodt*, G. Steyl

Department of Chemistry and Strategic Academic Cluster: Materials and Nanosciences, University of the Free State, Bloemfontein 9300, South Africa

ARTICLE INFO

Article history:

Received 1 September 2012

Accepted 29 October 2012

Available online 5 November 2012

Keywords:

β -Diketonato

Platinum(II)

Crystallography

DFT

Spectroscopy

Cyclooctadiene

Crystal structures

Venus fly-trap angles

ABSTRACT

Synthetic, structural and theoretical studies of Pt(II) complexes of a series of β -diketonato ligands with a variation of sterics, namely acetylacetonato (acac) and thenyltrifluoroacetato (thtfac), are reported. The crystal structures of [Pt(cod)(acac)]PF₆(I), [Pt(cod)(acac)]BF₄(II) and [Pt(cod)(thtfac)]BF₄(III) are presented while the complexes were characterized spectroscopically by IR, ¹H and ¹³C NMR spectroscopy. DFT calculations of the group 10 transition metals in the nickel triad, utilising the model complex, [M(cod)(acac)]⁺, to gain further insights in the variation of the transition metal within the complex and the interactions with both the β -diketonato and *cis,cis*-1,5-cyclo-octadiene (cod) co-ordinating ligands are reported. In particular, the variation in the ‘Venus fly-trap’ bite and jaw dihedral angles, χ and ψ , is *ca.* 2° and 4°, respectively, and therefore quite small, but significant. The HOMO and LUMO energy gaps between the Ni(II) and Pd(II) complexes were insignificant, while that of Pt(II) is >1 eV higher than the corresponding 3rd and 4th row congener complexes.

© 2012 Elsevier Ltd. All rights reserved.

1. Introduction

Diolenes act as ligands for a large number of metal centres and forms an important range of complexes for the study of π -bonding interactions. Bidentate olefins can also act as inhibitors in certain homogeneous catalytic processes and a more detailed knowledge on the bonding modes therein maybe exploited by more detailed and systematic variation of effects, which influences transition metal interactions therewith [1]. Similarly, classic β -diketonato and related ligands have been studied for more than a century and their ability to give rise to rich and interesting co-ordination chemistry is well known. β -Diketonato ligand systems act as monovalent *O,O'*-chelating donors capable of stabilizing mononuclear transition metal complexes. These *O,O'*-bidentate ligands may be underutilised in middle and late transition metal complexes [2], to evaluate dynamics and reaction mechanisms [3] as well as potential application in radiopharmaceuticals [4,5] and homogeneous catalysis [6–12]. The keto-enol tautomerism of this class of ligand has been widely studied [13,14]. The stepwise and subtle systematic ligand manipulation ability of β -diketonato ligand systems therefore allow investigation into the bonding modes and co-ordination of *cis,cis*-1,5-cyclo-octadiene (cod).

For these reasons we have focused our investigation to well known β -diketonato ligands which were commercially available (acetylacetonato (Hacac) and thenyltrifluoroacetato (Hthtfac)). In this paper we present the crystal structure of several β -diketonato cod platinum(II) complexes of the type [Pt(cod)(LL'-Bid)]A (where LL'-Bid = acac, thtfac; A = BF₄⁻, PF₆⁻) along with theoretical calculations on the [M(cod)(acac)]⁺ complex for the nickel triad. The aim is the further understanding of the co-ordination of a model diolefin ligand such as 1,5-cyclo-octadiene and the influence that the β -diketonato systems, while varying different counter ions, have on the respective structures and comparing the data for the cod ligand with the previously defined ‘Venus fly-trap’ bite and jaw dihedral angles, χ and ψ , [15] and a simultaneous evaluation of spectroscopic data.

2. Experimental

2.1. Materials and general procedures

All reagents used for synthesis and characterization were of analytical grade, purchased from Sigma–Aldrich, unless otherwise stated. Reagents were used as received, without purification.

NMR spectra were recorded on a Bruker Advance II 600 (¹H: 600.28 MHz; ¹³C: 150.96 MHz), ¹H NMR spectra were referenced internally using residual protons in the deuterated solvent

* Corresponding author.

E-mail address: roodta@ufs.ac.za (A. Roodt).

(CDCl₃: d 7.28; CD₂Cl₂: s 5.32). ¹³C NMR spectra were similarly referenced internally to the solvent resonance (CDCl₃: t 77.36; CD₂Cl₂: m 53.8) with values reported relative to tetramethylsilane (d 0.0). Chemical shifts are reported in ppm.

Infrared spectra were recorded on a Bruker Tensor 27 Standard System spectrophotometer with a laser range of 4000–370 cm⁻¹. Solid samples were prepared as potassium bromide disks.

Preparation of dichlorido-1,5-cyclo-octadieneplatinum(II) starting material was achieved by the previously published method [16] from the reaction of potassium tetrachloroplatinate in water and propanol with *cis,cis*-1,5-cyclo-octadiene (cod).

2.2. Synthesis

2.2.1. Preparation of [Pt(cod)(acac)]PF₆(I) and [Pt(cod)(acac)]BF₄(II)

[Pt(cod)Cl₂] (100 mg, 0.27 mmol) was dissolved in dichloromethane (5 ml). To this AgA (A = PF₆, BF₄, 135.1 mg or 104.1 mg 0.53 mmol) was added, the resulting solution was stirred for ca. 15 min. An equivalent of acetylacetonate (Hacac, 27 mg, 0.27 mmol) was added and the mixture stirred for a few minutes to allow the reaction to complete. The solution was filtered and diethyl ether was added to the filtrate to precipitate the product. The resulting solution was again filtered and the precipitate washed with diethyl ether. Crystals suitable for X-ray determination were obtained by DCM/Et₂O vapour diffusion.

Yield (I) 42 mg (53%); (II) 100 mg (74%).

I: IR_{KBr}: ν_{C=C} 1526, ν_{C=O} 1556, ν_{Pt-O} 647 and 473, ν_{Pt-[C=C]} 558 cm⁻¹. ¹H NMR (600.28 MHz, CD₂Cl₂) δ 2.008 (s, 6H, CH₃), 2.492 (q, 4H, CH₂), 2.836 (d, 4H, CH₂), 5.744 (t, 4H, CH), 5.861 (s, 1H, CH). ¹³C NMR (150.96 MHz, CD₂Cl₂) δ 26.70 (CH₃), 29.95 (CH₂), 99.51 (CH), 103.02 (CH), 187.84 (CO).

II: IR_{KBr}: ν_{C=C} 1529, ν_{C=O} 1555, ν_{Pt-O} 645 and 474, ν_{Pt-[C=C]} 521 cm⁻¹. ¹H NMR (600.28 MHz, CD₂Cl₂) δ 2.209 (s, 6H, CH₃), 2.499 (q, 4H, CH₂, **IIa**), 2.254 (q, 4H, CH₂, **IIb**), 2.683 (dd, 4H, **IIb**), 2.841 (d, 4H, CH₂, **IIa**), 5.556 (t, 4H, CH, **IIb**), 5.75 (t, 4H, CH, **IIa**), 5.862 (s, 1H, CH). ¹³C NMR (150.96 MHz, CD₂Cl₂) δ 26.81 (CH₃), 29.97 (CH₂, **IIa**), 31.23 (CH₂, **IIb**), 99.53 (t, CH, **IIa**), 100.94 (CH, **IIb**), 103.02 (CH), 187.81 (CO).

2.2.2. Preparation of [Pt(cod)(thtfac)]BF₄(III)

Using the preparation method presented in Section 2.2.1, changing the β-diketonato ligand to thenoyltrifluoroacetone (Hthtfac) complex **III** was synthesized. Crystals suitable for X-ray determination were obtained by DCM/Et₂O vapour diffusion.

Yield (**III**) 90 mg (54%).

III: IR_{KBr}: ν_{C=C} 1540, ν_{C=O} 1579, ν_{Pt-O} 613 and 473, ν_{Pt-[C=C]} 522 cm⁻¹. ¹H NMR (600.28 MHz, CDCl₃) δ 2.604 (m, 4H, CH₂), 2.727 (m, 4H, CH₂), 5.626 (t, 4H, CH), 6.717 (s, 1H, CH), 7.969 (d, 1H, CH), 8.085 (d, 2H, CH). ¹³C NMR (150.96 MHz, CDCl₃) δ 30.22 (CH₂), 31.28 (CH₂), 100.42 (t, CH), 120.94 (CH), 130.59 (CH), 136.72 (CH), 139.73 (CF₃), 198.87 (CO).

2.3. X-ray crystallographic data collection and refinement

Data collections for [Pt(cod)(acac)]PF₆(I) was obtained on a Bruker APEX II 4K CCD diffractometer. The data for [Pt(cod)(acac)]BF₄(II) and [Pt(cod)(thtfac)]BF₄(III) were collected on an Oxford Diffraction Xcalibur 3 CrysAlis CCD system [17]. Both systems were equipped with a graphite-monochromated Mo Kα radiation, for the Bruker system all the reflections were merged and integrated with SAINT-PLUS [18] and corrected for Lorentz, polarization and absorption effects with SADABS [19], while CrysAlis RED [20] was used for the Oxford Diffraction system.

Structures were solved by direct and conventional Patterson methods using SHELX-97 [21] as part of the WINGX [22] package, and anisotropic refinement was performed on all non-hydrogen

atoms by a full-matrix least-squares method. The positions of the hydrogen atoms were calculated using a riding model to the adjacent carbon, unless otherwise stipulated. Hydrogen interactions were calculated using the PLATON [23–25] and PARST [26] programs. Molecular graphics were obtained using DIAMOND [27], while overlay illustrations were generated using HyperChem™ 7.5 [28].

Details of the crystal data, intensity measurements and data processing are summarized in Table 1 for [Pt(cod)(acac)]PF₆(I), [Pt(cod)(acac)]BF₄(II) and [Pt(cod)(thtfac)]BF₄(III) while selected bond distances and angles are given in Table 2. The molecular structure with thermal ellipsoids at 50% probability and numbering scheme for complex **I** are shown in Fig. 1, complex **II** is likewise numbered, the counter-ions and hydrogen atoms have been omitted for clarity. The numbering scheme of complex **III** is represented in Fig. 2, crystallizing with two independent complexes in the asymmetric unit, labelled as **IIIa** and **IIIb**, respectively. The atoms are prefixed with 1 or 2, respectively, e.g. O₁₁ and O₂₁ for the first oxygen atom of the β-diketonato ligand, and again the counter-ions and hydrogen atoms have been omitted for clarity.

2.4. Computational methodology

The DFT (density functional theory) molecular orbital calculations were carried out using the GAUSSIAN 03 [29] software suite. Becke's three parameter hybrid (B3LYP) [30,31] exchange correlation functional was used. The basis set employed in this study was 6-311++G(d,p) [32–34] for the main group elements and LanL2DZ [35] for the middle to late transition metals. Vibrational frequencies were calculated at the 6-311++G(d,p) level for the main group elements and at the LanL2DZ level for the middle to late transition metals with minimum energies confirmed to have zero imaginary frequencies. The frequencies were unscaled and used to compute the zero-point vibrational energies, while the calculated harmonic wavenumbers were used in the analysis of the experimental IR spectra. The values were scaled down by the factor 0.9982, to account for anharmonicity effects and limitations of the basis set [36].

3. Results and discussion

3.1. Synthesis and characterization

The platinum(II) complexes (**I–III**) were synthesized utilising potassium tetrachloroplatinate in a mixture of water and propanol followed by the addition of a catalytic amount of tin chloride and an excess of *cis,cis*-1,5-cyclo-octadiene (cod). The mixture was stirred for several days and allowed to evaporate to dryness where upon it was extracted with dichloromethane. The resulting dichloro(1,5-cyclo-octadiene)platinum(II) complex was then further reacted with an equivalent of the β-diketonato ligand in the presence of a silver salt (Scheme 1). The compounds described in this paper were characterized by IR, ¹H and ¹³C NMR spectroscopy (data in Section 2.2).

The IR spectra of the compounds showed characteristic bands at 613–647 cm⁻¹ and ± 474 cm⁻¹ assigned to ν_{Pt-O} + Δring (in-plane ring distortion) and ν_{Pt-O} while ν_{Pt-[C=C]} bands were observed around 558–521 cm⁻¹. These bands were assigned based on the previous assignments of similar compounds by Mikami et al. [37] and Nakamoto et al. [38] who studied a range of bis-acetylacetonato transition metal complexes. The O–Pt–O bite angle decreases when varying the β-diketonato ligands from acac to thtfac leading to an increase in strain on the metallocycle, this is seen in the IR by ca. 34 cm⁻¹ shift down-field.

The ¹H NMR data is given in Section 2.2 and the complexes have been described considering the atomic numbering scheme given in

Table 1
Crystallographic data and refinement parameters for [Pt(cod)(LL'-Bid)]A, where A = PF₆⁻ and BF₄⁻, LL'-Bid = acac, thtfac.

| Crystal data | [Pt(cod)(acac)]A | | [Pt(cod)(thtfac)]A |
|--|--|---|--|
| | PF ₆ ⁻ (I) | BF ₄ ⁻ (II) | BF ₄ ⁻ (III) |
| Empirical formula | C ₁₃ H ₁₉ F ₆ O ₂ Pt | C ₁₃ H ₁₉ BF ₄ O ₂ Pt | C ₁₆ H ₁₆ BF ₄ O ₂ PtS |
| Formula weight | 547.34 | 489.18 | 611.25 |
| T (K) | 100(2) | 100(2) | 100(2) |
| λ (Å) | 0.7103 | 0.71073 | 0.7103 |
| Crystal system | monoclinic | orthorhombic | monoclinic |
| Space group | P2 ₁ /c | Pca2 ₁ | P2 ₁ /c |
| Unit cell dimensions | | | |
| a (Å) | 9.3082(3) | 26.3980(4) | 14.4456(2) |
| b (Å) | 15.4486(5) | 7.19670(10) | 15.1804(1) |
| c (Å) | 12.6335(3) | 7.71820(10) | 19.5643(3) |
| α (°) | 90 | 90 | 90 |
| β (°) | 119.164(2) | 90 | 117.551(1) |
| γ (°) | 90 | 90 | 90 |
| V (Å ³) | 1586.38(8) | 1466.29(4) | 3803.74(8) |
| Z | 4 | 4 | 8 |
| D _{calc} (Mg m ⁻³) | 2.292 | 2.216 | 2.135 |
| Absorption coefficient (mm ⁻¹) | 9.013 | 9.613 | 7.563 |
| F(000) | 1040 | 928 | 2320 |
| Crystal size (mm) | 0.39 × 0.22 × 0.12 | 0.26 × 0.18 × 0.03 | 0.51 × 0.26 × 0.13 |
| Theta range for data collection (°) | 3.22 to 28.38 | 2.83 to 27.98 | 2.53 to 28.00 |
| Index ranges | -12h ≤ 10, -20 ≤ k ≤ 18, -16 ≤ l ≤ 16 | -34 ≤ h ≤ 34, -9 ≤ k ≤ 7, -10 ≤ l ≤ 8 | -19 ≤ h ≤ 19, -20 ≤ k ≤ 11, -25 ≤ l ≤ 25 |
| Reflections collected | 15026 | 11111 | 29977 |
| Independent reflections | 3963 [R _{int} = 0.0479] | 2884 [R _{int} = 0.0233] | 9095 [R _{int} = 0.0333] |
| Completeness to θ (°; %) | 28.38, 99.4 | 27.98, 99.4 | 28.00, 99.1 |
| Maximum and minimum transmission | 0.411 and 0.127 | 0.761 and 0.189 | 0.440 and 0.113 |
| Refinement method | Full-matrix least-squares on F ² | Full-matrix least-squares on F ² | Full-matrix least-squares on F ² |
| Data/restraints/parameters | 3963/0/210 | 2884/1/186 | 9095/0/505 |
| Goodness-of-fit on F ² | 1.037 | 1.054 | 0.947 |
| Final R indices [I > 2σ(I)] | R ₁ = 0.0286, wR ₂ = 0.0558 | R ₁ = 0.0175, wR ₂ = 0.0439 | R ₁ = 0.0257, wR ₂ = 0.0554 |
| R indices (all data) | R ₁ = 0.0406, wR ₂ = 0.0597 | R ₁ = 0.0195, wR ₂ = 0.0445 | R ₁ = 0.0387, wR ₂ = 0.0591 |
| Largest difference in peak and hole (e Å ⁻³) | 1.431 and -1.369 | 1.468 and -0.721 | 1.964 and -1.270 |

Table 2
Selected experimental and optimised bond distances (Å) and angles (°) for complexes I–III.

| | I | II | Calc ^a | IIIa | IIIb |
|-----------------------------------|----------|----------|-------------------|----------|----------|
| Pt–O ₁ | 2.011(3) | 2.015(3) | 2.041 | 2.011(3) | 2.007(3) |
| Pt–O ₂ | 2.009(3) | 2.013(3) | 2.041 | 2.015(3) | 2.025(3) |
| Pt–C ₁ | 2.161(4) | 2.160(3) | 2.221 | 2.152(4) | 2.151(4) |
| Pt–C ₂ | 2.146(4) | 2.153(4) | 2.205 | 2.166(4) | 2.165(4) |
| Pt–C ₅ | 2.148(5) | 2.164(3) | 2.221 | 2.152(4) | 2.152(4) |
| Pt–C ₆ | 2.154(4) | 2.147(4) | 2.205 | 2.157(4) | 2.161(4) |
| C ₁ –C ₂ | 1.401(6) | 1.388(8) | 1.399 | 1.395(5) | 1.398(5) |
| C ₅ –C ₆ | 1.393(6) | 1.411(8) | 1.399 | 1.392(5) | 1.399(5) |
| O ₁ –Pt–O ₂ | 93.5(1) | 93.5(1) | 91.95 | 92.4(1) | 92.8(1) |
| C ₁ –Pt–C ₂ | 38.0(2) | 37.6(2) | 36.84 | 37.7(1) | 37.8(1) |
| C ₅ –Pt–C ₆ | 37.8(2) | 38.2(2) | 36.84 | 37.7(1) | 37.9(1) |
| C ₁ –Pt–C ₆ | 82.3(1) | 82.2(2) | 81.41 | 82.9(1) | 82.1(1) |
| C ₂ –Pt–C ₅ | 82.3(1) | 82.0(2) | 81.41 | 88.7(1) | 82.9(1) |
| χ ^b | 86.8(4) | 86.9(2) | 85.9 | 87.4(1) | 87.4(2) |
| ψ ^c | 78.9(5) | 79.1(2) | 82.1 | 78.9(2) | 80.5(2) |

^a Calculated [Pt(cod)(acac)]⁺ moiety.

^b See below for definition of χ and ψ.

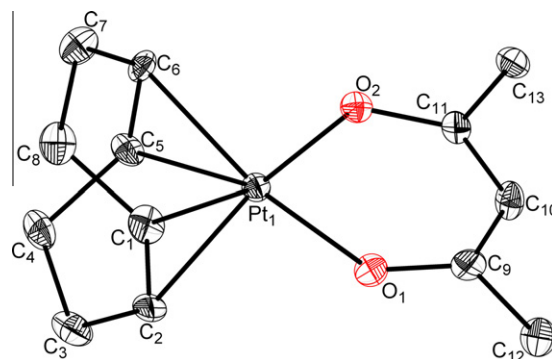


Fig. 1. The molecular structure of I. Displacement ellipsoids are drawn at 50% probability. Hydrogen atoms and counter ion have been omitted for clarity.

for complex II but was not present in complexes I and III; this was ascribed to the folding of the cod in solution. The ¹³C{¹H} NMR resonances (data in Section 2.2), including the Pt satellites, were in accordance with the proposed structures.

3.2. Structural description

The platinum metal centres of complexes I–III are bonded to the two oxygen atoms of the β-diketonato ligands and π-bonded with the alkene bonds of the *cis,cis*-1,5-cyclo-octadiene (cod) ligand giving rise to a square planar co-ordination geometry around the metal centre. A low temperature re-determination of II at 100 K was

Fig. 1. The resonances of methine hydrogen atoms of the cod demonstrated the classic triplet of ¹⁹⁵Pt coupling [³J_{Pt-H} = 33 Hz]. With a singlet observed for the β-diketonato hydrogen (H₁₀), for complex III a shift higher field (6.71 ppm) was found as a result of the additional electron withdrawing of the substituents of the thtfac ligand. Both complexes I and II showed similar shifts (5.86 ppm) leading to the conclusion that the counter ions do not play a significant role in the cationic species. A rotamer was found

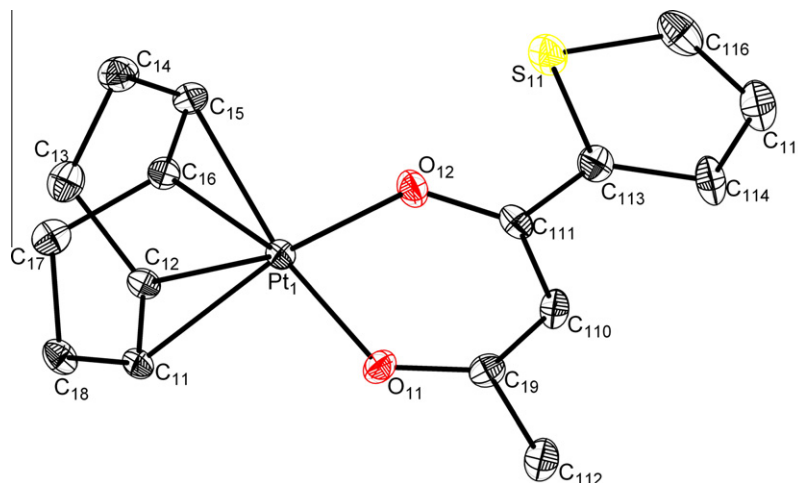
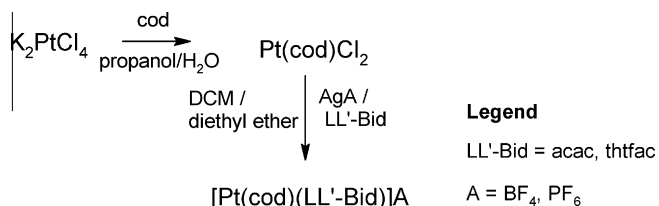


Fig. 2. The molecular structure of **IIIa**. Displacement ellipsoids are drawn at 50% probability. Hydrogen atoms and counter ion have been omitted for clarity.



Scheme 1. Synthesis of the platinum(II) cyclo-octadiene β -diketonato complexes.

done (original by Venkatasubramanian [39]), to ensure accurate data and thus allowing for the direct comparison with complex **I**. Due to the cationic nature of the complexes the resulting charge is balanced with either the hexafluorophosphate (PF_6^-) or tetrafluoroborate (BF_4^-) counter-ions. The ions display classic distorted tetragonal (BF_4^-) and octahedral (PF_6^-) co-ordination geometries with no disorder present. The varying of the counter-ion does not significantly change the bond distances observed for the platinum centre, nor the general coordination mode, see Table 2. Moreover, the variation of the solid state packing mode and intermolecular packing effects proved to be negligible. The alkene ($\text{C}=\text{C}$) bond lengths of cod were not affected by the increased electron withdrawing groups on the *trans* acac-type ligand and generally remained constant with a mean value of 1.397(6) Å.

The distortion from square planar geometry as measured by the intersection of the planes defined by the mid-point of the alkene carbons of the cod ring with the oxygen atoms of the β -diketonato and the platinum metal centre with the β -diketonato back-bone is as follows: complex **IIIa** > **IIIb** > **II** > **I** being 5.48(5)°, 4.77(5)°, 4.19(6)° and 2.57(6)°, respectively.

The hydrogen interactions for complex **I** and **II** originate mostly between the cod moieties and the counter-ions. However, hydrogen bond interactions with the β -diketonato moieties are present as listed in Table 3 and illustrated in Fig. 3. For both complex **I** and **II** the different fluorido ligands on the BF_4^- counter ion (F_3) is split between the methine hydrogen (H_{10}) and the methyl hydrogen (**I**: $\text{H}_{12\text{B}}$ and **II**: $\text{H}_{13\text{B}}$) atoms. An additional 'splitted' fluorido ligand interaction (F_4) is observed for **II**. For complex **I** a further interaction with the cod moiety with the fluorido ligand (F_5) was found.

Due to variations in the hydrogen interactions, crystal system and the presence of metal chelate ring interactions (Fig. 4) the packing of **I** was found to be a clustered head-to-tail whilst a classic head-to-tail packing for **II** was seen (Supplementary data). The

metal chelate ring interactions of the platinum co-ordinated acetylacetonato metallocycle between the metal chelate ring and the methine (H_{10}) hydrogen of the acac moiety are illustrated in Fig. 4 and exhibit distances of 3.5804 Å with symmetry operator $3/2 - x, y, 1/2 + z$, while the methyl ($\text{H}_{12\text{C}}$)-metal chelate ring has a distance of 2.762 Å.

3.3. Computational data

No accurate relevant solid state data for isostructural complexes of all members of the nickel triad are available to enable comparison for the different metal centres since isolation of suitable and stable crystals proved to be a significant challenge. Thus, DFT calculations were performed to compare the geometry with that obtained from the solid state studies, gain insight into the electronic structures and explain the bonding nature and spectral properties of the complexes. An excellent correlation between the computed structures and that of the experimental structures was obtained as can be seen in Fig. 5, which presents the HyperChem™ superimposed image of complexes **I** and **II** with the calculated $[\text{Pt}(\text{cod})(\text{acac})]^+$ moiety with *r.m.s.* values of 0.067 and 0.076 Å, respectively. In general, the optimised geometric parameters are in very good agreement with the values based upon the X-ray crystal structure data as can be seen in Table 2, and the common trends observed in the experimental data are excellently reproduced in the calculations. It should be noted that the theoretical calculations do not consider the effects of the chemical environment for example intra- and intermolecular packing interactions. As a result the distances for the theoretical calculations are fractionally larger (1–3%) than those observed for the X-ray crystal structures.

In the calculated IR spectrum of $[\text{Pt}(\text{cod})(\text{acac})]^+$ moiety with the experimental spectra of complexes **I** and **II** are graphically displayed, while selected vibrations are presented in the Supplementary material (Fig. S5, Table S2); with no deconvolution of experimental bands performed. Therefore, the number of IR signals shown by the theoretical spectrum of a given complex may be larger with respect to that shown by the experimental spectrum of the same complex.

The PF_6^- anion stretching frequencies are found in the region between 920 and 740 cm^{-1} while that of the BF_4^- is located at 980–1150 cm^{-1} . The strongest bands of the experimental spectra were assigned as the anions, for complex **II** the BF_4^- anion bands were found at 1097, 1057, 1038 and 1011 cm^{-1} representing the four $\nu_{\text{B-F}}$ frequencies, while for complex **I** the PF_6^- anion was seen

Table 3
Hydrogen bond distances and angles for complexes **I–II** [Å and °].

| D–H...A | d(D–H) | d(H...A) | d(D...A) | ∠(DHA) |
|---|----------------------------|---------------------------------|----------|--------|
| I | | | | |
| C ₅ –H ₅ ...F ₅ | 0.98 | 2.37 | 3.140(6) | 135.5 |
| C ₇ –H _{7A} ...F ₄ ^{#1} | 0.97 | 2.52 | 3.332(6) | 140.8 |
| C ₂ –H ₂ ...F ₃ ^{#2} | 0.98 | 2.53 | 3.360(5) | 142.8 |
| C ₆ –H ₆ ...F ₆ ^{#3} | 0.98 | 2.48 | 3.242(5) | 134.7 |
| C ₁₂ –H _{12B} ...F ₃ ^{#4} | 0.96 | 2.55 | 3.432(6) | 152.6 |
| C ₁₀ –H ₁₀ ...F ₃ ^{#4} | 0.93 | 2.39 | 3.271(5) | 158.7 |
| II | | | | |
| C ₂ –H ₂ ...F ₁ | 1.00 | 2.54 | 3.255(6) | 128.1 |
| C ₂ –H ₂ ...F ₃ | 1.00 | 2.47 | 3.145(6) | 123.9 |
| C ₃ –H _{3B} ...F ₄ ^{#5} | 0.99 | 2.39 | 3.320(7) | 156.5 |
| C ₇ –H _{7A} ...F ₂ ^{#6} | 0.99 | 2.40 | 3.266(7) | 146.2 |
| C ₆ –H ₆ ...F ₄ ^{#7} | 1.00 | 2.31 | 3.192(6) | 146.7 |
| C ₁₃ –H _{13C} ...F ₁ ^{#7} | 0.98 | 2.65 | 3.609(6) | 166.0 |
| C ₇ –H _{7B} ...F ₁ ^{#8} | 0.99 | 2.55 | 3.360(7) | 138.7 |
| C ₁₂ –H _{12B} ...F ₄ ^{#9} | 0.98 | 2.48 | 3.445(5) | 166.9 |
| C ₁₀ –H ₁₀ ...F ₃ ^{#9} | 0.95 | 2.44 | 3.328(5) | 156.5 |
| C ₁₃ –H _{13B} ...F ₃ ^{#9} | 0.98 | 2.48 | 3.368(6) | 151.2 |
| Symmetry transformations used to generate equivalent atoms | | | | |
| #1 – x, y – 1/2, –z + 3/2 | #2x, –y + 1/ 2, z + 1/2 | #3x – 1, –y + 1/2, z – 1/2 | | |
| #4 – x + 1, y – 1/2, –z + 3/2 | #5x, y – 1, z | #6 – x + 1, –y + 1, z – 1/2 | | |
| #7x, y – 1, z – 1 | #8x, y, z – 1 | #9 – x + 3/2, y – 1, z – 1/2 | | |

at 842 cm⁻¹ a single band was observed due to the octahedral symmetry (O_h) of the anion.

Due to the conjugation present in the β-diketonato back-bone the ν_{C=O} bands were expected at a lower wavenumber region than for the standard ketone frequencies (1725–1705 cm⁻¹), with an

additional expected decrease compared to an uncoordinated β-diketone ligand. For complex **I** and **II** nearly identical values of 1556 cm⁻¹ were obtained with the computed value in good agreement with the assignment. A similar lowering of the frequencies due to the conjugation for ν_{C=C} was also found with values of 1526 cm⁻¹ for **I** and 1529 cm⁻¹ for **II**, respectively. Of further interest in this study are the ν_{Pt–O} and ν_{Pt–[C=C]} frequencies describing the co-ordination environment of the platinum metal centre. Moreover, it is noted that the counter-ion neither plays a significant role in the co-ordination polyhedron's geometry, nor does the hydrogen interactions found between the cod and β-diketonato back-bone and the counter-ions significantly alter the harmonics.

An additional weak band at ± 1350 cm⁻¹ observed in the experimental data (Supplementary data Fig. S5) may be attributed to ν_{as} of the conjugated ketones of the acetylacetonato ligands. For the computed spectra this stretching harmonic is combined with the wagging (ω) of the methylene (CH₂) groups of the cod moiety as illustrated in Fig. 6, resulting in a broader band.

In the comparison of the different calculated IR spectra the unscaled values were used (Table 4). It is clear from the discussion above that the scaled values are in good agreement with the experimentally observed bands (Supplementary data Fig. S5 and Table S2). Small changes with maximum differences of 8 cm⁻¹, to the symmetrical stretching frequency of the co-ordinated conjugated ketone functionality of the acetylacetonato moiety (ν_{C=O}) was observed, while the largest variation was found for the ν_{C=C} acac ligand with a variation of 14 cm⁻¹ when varying the group 10 metal centre as presented in Fig. 6.

Two geometric angles are specifically highlighted in this investigation, namely the chi (χ) or 'bite' angle characterized by the intersection of the planes, defined by adjacent alkene carbons of the cod ligand and the platinum metal centre. Secondly, the psi (ψ) or 'jaw' angle characterized by the intersection between planes

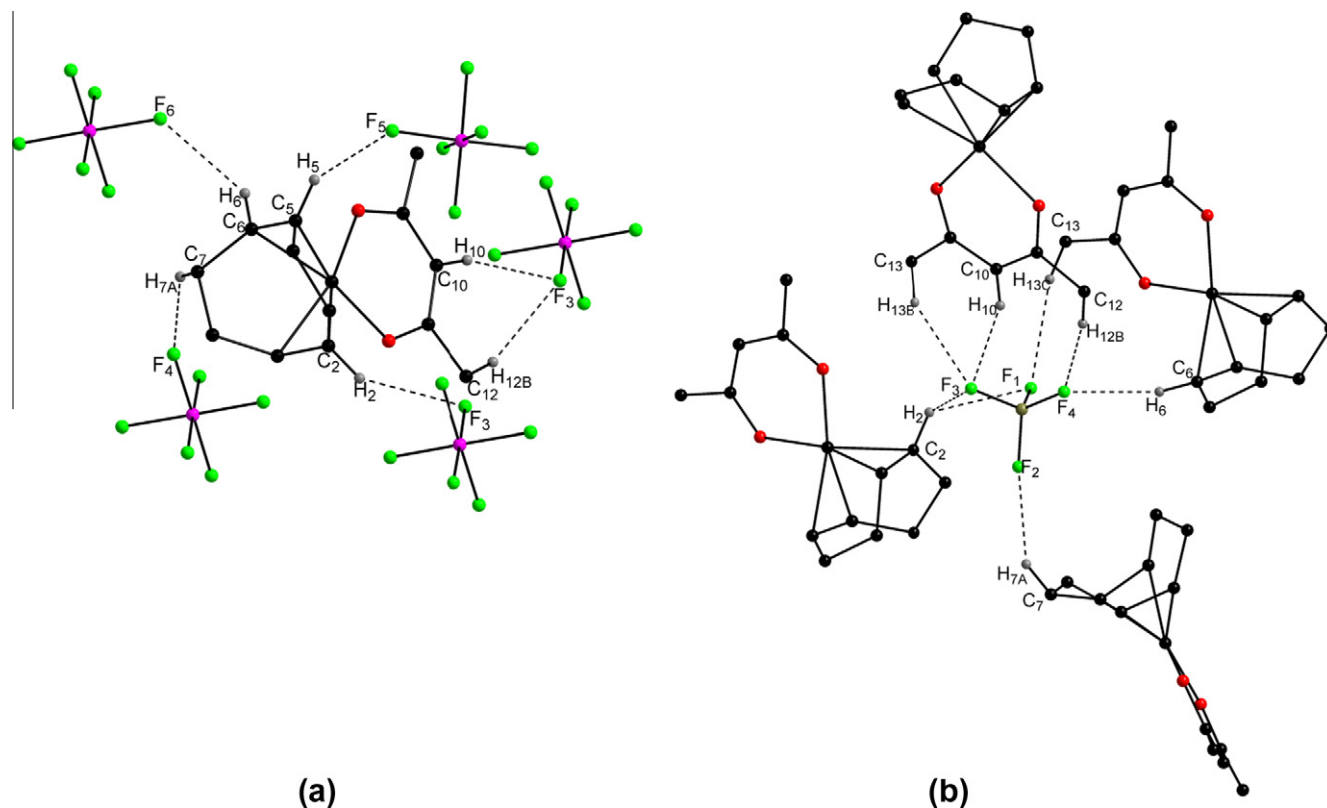


Fig. 3. Molecular diagram of (a) **I** and (b) **II** illustrating hydrogen interactions by a dashed bond. Only relevant hydrogen atoms have been included.

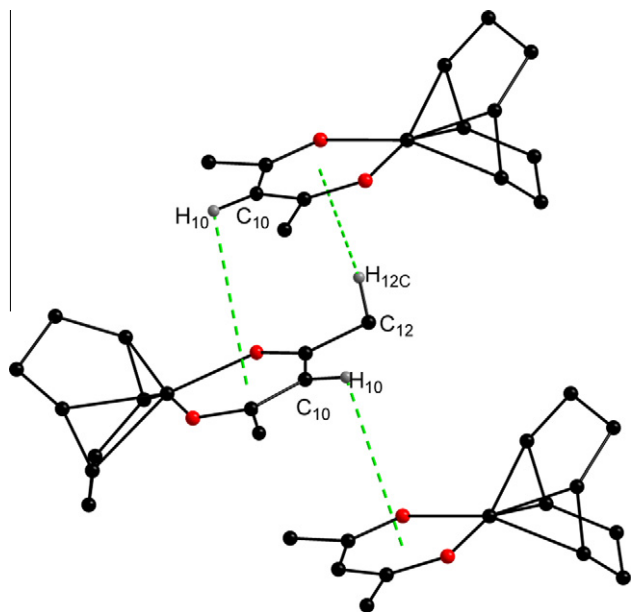


Fig. 4. Molecular diagram of **II** illustrating metal chelate ring interactions by dashed bonds. Only selected hydrogen atoms are included; tetrafluoroborate counter ions omitted for clarity. Symmetry operators $[3/2 - x, y, 1/2 + z]$ and $[1/2 - x, y, -1/2 + z]$.

Table 4

Selected calculated IR (cm^{-1}), χ ($^\circ$) and ψ ($^\circ$) values for the Group 10 metal complexes. Unscaled.

| | $[\text{Ni}(\text{cod})(\text{acac})]^+$ | $[\text{Pd}(\text{cod})(\text{acac})]^+$ | $[\text{Pt}(\text{cod})(\text{acac})]^+$ |
|---------------------------------|--|--|--|
| $\nu_{\text{C}=\text{O}}$ | 1577 | 1569 | 1572 |
| $\nu_{\text{C}=\text{acac}}$ | 1553 | 1543 | 1557 |
| $\nu_{\text{C}=\text{Ccod}}$ | 1605 w | 1567 w | 1541 w |
| $\nu_{\text{as C}=\text{Ccod}}$ | 1593 w | 1559 w | 1531 w |
| $\nu_{\text{as C}=\text{O}}$ | 1377 | 1378 | 1384 |
| χ^a | 86.6 | 84.8 | 85.9 |
| ψ^a | 85.9 | 84.9 | 82.1 |

^a See Fig. 7 for definition of χ and ψ .

defined by the alkane carbons of the cod moiety, as depicted graphically in Fig. 7.

By comparing the crystallographic and computed values of the ‘jaw’ and ‘bite’ angles, for **I** and **II** with $[\text{Pt}(\text{cod})(\text{acac})]^+$ (Table 2) it was observed that the values remain similar, with a few degrees difference detected.

Upon descending the Ni-triad the theoretical values (Table 4) for the ‘bite’ angle follow a similar trend to the covalent radii of the triad, namely $\text{Ni} < \text{Pt} < \text{Pd}$, whilst the ‘jaw’ angle closes as one proceeds down the triad with a difference of ca. 3.8° from top to bottom, and clearly represents quite a small change. This is quite interesting since, upon variation of the electronic properties of the trans bidentate acac type ligand for the Pd(**II**) only, a significant effect in the jaw angle of up to 8 degrees was observed [15]. Expansion of the use of the jaw and bite angles in follow-up

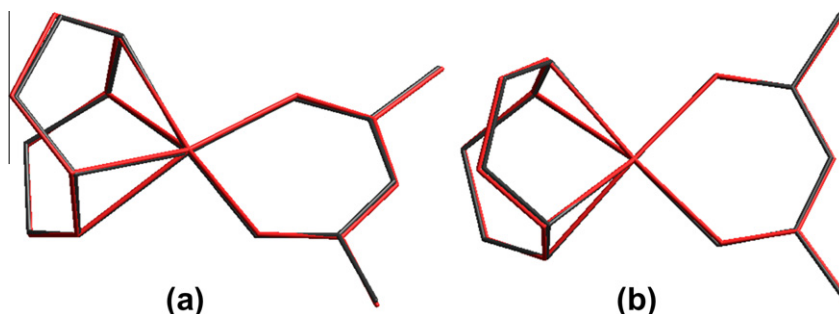


Fig. 5. HyperChem™ superimposed image of (a) $[\text{Pt}(\text{cod})(\text{acac})]\text{BF}_4(\text{II})$ (black) vs. $[\text{Pt}(\text{cod})(\text{acac})]^+$ (calculated) (red) with an RMS error of 0.067 Å (b) $[\text{Pt}(\text{cod})(\text{acac})]\text{PF}_6(\text{I})$ (black) vs. $[\text{Pt}(\text{cod})(\text{acac})]^+$ (calculated) (red) with an RMS error of 0.076 Å. The counter-ions and hydrogen atoms of the X-ray crystal structures have been omitted for clarity. (For interpretation of the references to colour in this figure legend, the reader is referred to the web version of this article.)

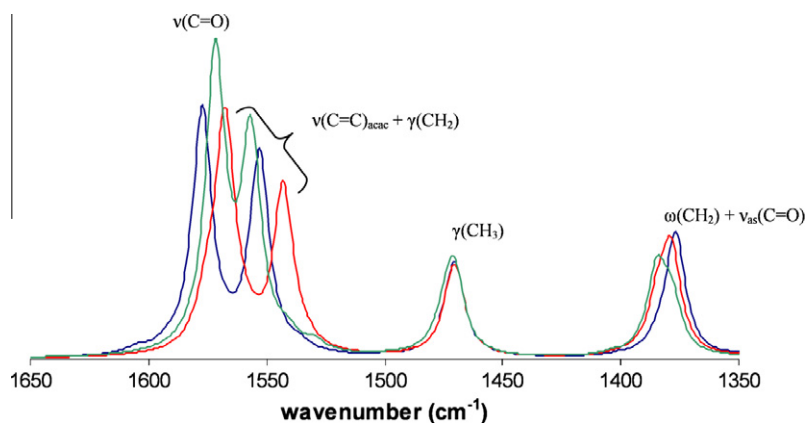


Fig. 6. Calculated IR spectrum of the finger print region of $[\text{Ni}(\text{cod})(\text{acac})]^+$ (blue), $[\text{Pd}(\text{cod})(\text{acac})]^+$ (red) and $[\text{Pt}(\text{cod})(\text{acac})]^+$ (green). ν – stretching, γ – rocking, scissoring, ω – wagging; unscaled. (For interpretation of the references to colour in this figure legend, the reader is referred to the web version of this article.)

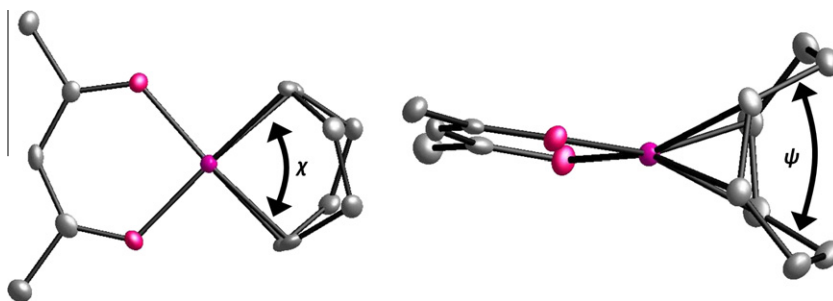


Fig. 7. Left, the interplanar bond angle χ , the 'bite' of the Venus fly-trap, formed by the olefinic moieties through the platinum metal centre. Right, the extent of the opening of the Venus fly-trap 'jaw' angle, ψ , as defined by the planes through the alkane carbons of the cyclo-octadiene moiety.

Table 5
Molecular orbitals of calculated structures $[M(\text{cod})(\text{acac})]^+$.

| | HOMO–1 | HOMO | LUMO | LUMO+1 |
|--------|--------|------|------|--------|
| Ni(II) | | | | |
| Pd(II) | | | | |
| Pt(II) | | | | |

investigations are therefore paramount in defining the diolefinic coordination in these cod systems more accurately.

The visual representation of the molecular orbitals (MOs) is another method whereby interactions of the cyclo-octadiene with the various metal centres and the *trans* β -diketonato ligand may be observed. The second-highest (HOMO–1) and highest (HOMO) occupied MOs and the lowest (LUMO) and second-lowest (LUMO+1) unoccupied MOs for the calculated complexes of $[M(\text{cod})(\text{acac})]^+$ where $M = \text{Ni}, \text{Pd}, \text{Pt}$ (group 10 metals) are presented in Table 5 and Table 6, along with the differences in the respective orbitals ($E_{g-1} \equiv \Delta|\text{HOMO}-1| - |\text{HOMO}|$; $E_g \equiv \Delta|\text{HOMO}| - |\text{LUMO}|$; $E_{g+1} \equiv \Delta|\text{LUMO}| - |\text{LUMO}+1|$). The contour plots shown with the MOs in Table 5 are viewed along the z-axis. The gap energies reflect the chemical activity of the molecules ability of the MOs to donate (HOMO) or accept (LUMO) an electron.

Table 6
Molecular orbital energies (Hartree) and energy gaps (eV) of the $[M(\text{cod})(\text{acac})]^+$ ($M = \text{Ni}, \text{Pd}, \text{Pt}$) calculated structures.

| M(II) | Molecular orbital energies (Hartree) | | | | Energy Gaps (eV) | | |
|--------|--------------------------------------|----------|----------|----------|------------------|-------|-----------|
| | HOMO–1 | HOMO | LUMO | LUMO+1 | E_{g-1} | E_g | E_{g+1} |
| Ni(II) | –0.41512 | –0.37704 | –0.2485 | –0.19038 | 1.036 | 3.498 | 1.582 |
| Pd(II) | –0.41333 | –0.37277 | –0.24407 | –0.18711 | 1.104 | 3.502 | 1.550 |
| Pt(II) | –0.41536 | –0.37796 | –0.2089 | –0.19198 | 1.018 | 4.600 | 0.460 |

The HOMO–1 MOs of nickel and palladium are comparable with π orbital delocalization occurring between both the cyclo-octadiene moiety and the acetylacetonato moiety. Platinum however only shows delocalization between the metal and the

acetylacetonato moiety. For the HOMO MOs delocalization on the back-bone of the acetylacetonato moiety is seen for all three complexes, with the platinum complex showing some electron density around the cyclo-octadiene alkene carbons, with a d_{yz} orbital centred on the metals. A $d_{x^2-y^2}$ orbital contribution is observed on the metal centres for the LUMO MOs.

The MOs of the HOMO level illustrate the orbitals which are utilised for back bonding in the cyclo-octadiene ligand. The additional orbitals around the oxygen are capable of shared hydrogen/fluorine interactions. The back bonding of the nickel complex was found to be small whereas the palladium complex showed almost none. This capability of back bonding is assumed to be the reason why the platinum complexes are the most stable of the triad.

4. Conclusions

The synthesis, characterization and structure of new β -diketonato complexes of *cis,cis*-1,5-cyclo-octadiene Pt(II) have been reported. The contribution of both the counter ion interactions as well as the metal chelate ring interactions observed in **I** and **II** lead to the variation of packing from a clustered head-to-tail to a classic head-to-tail. In spite of variations in the solid state packing, an excellent agreement between the low temperature X-ray data collections and the computed structures was observed with *r.m.s.* values of *ca.* 0.07 Å, with reasonable correlations with bond lengths, angles and IR spectra were found. The ‘jaw’ and ‘bite’ angles for both the crystal structures and the computed structures were presented, leading to the conclusion that upon varying the metal centre in identical complexes down the Nickel triad and varying *only* the metal centre, the ‘jaw’ angle closes only slightly. The HOMO–LUMO energy gap from the nickel to the palladium essentially stays the same, whereas there is more than 1 eV increase from the Pd to the Pt. Further investigation into the ‘jaw’ and ‘bite’ angles, and the energy differences along the triads and periodically for various β -diketonates and transition metals will be essential to fully formulate the manipulation and understanding of the bonding modes of the cyclo-octadiene ligand.

Acknowledgements

Financial assistance from the University of the Free State under the Strategic Academic Cluster initiative (Materials and Nanosciences) is gratefully acknowledged as well as the use of the High Performance Cluster for the GAUSSIAN03 calculations. We thank Prof. Ola Wendt from the University of Lund, Sweden for the use of their Oxford X-ray diffractometer. We also express our gratitude to SASOL, the South African National Research Foundation (SA-NRF/THRIP) and the Swedish International Development Co-operation Agency (SIDA) for financial support of this project. Part of this material is based on work supported by the SA-NRF/THRIP under Grant No. GUN 2068915. Opinions, findings, conclusions or recommendations expressed in this material are those of the authors and do not necessarily reflect the views of the SA-NRF.

Appendix A. Supplementary material

CCDC 883760 (I), 883761 (II) and 883762 (III) contain the supplementary crystallographic data for this article. These data can be

obtained free of charge from The Cambridge Crystallographic Data Centre via www.ccdc.cam.ac.uk/data_request/cif. Supplementary data associated with this article can be found, in the online version, at <http://dx.doi.org/10.1016/j.poly.2012.10.043>.

References

- [1] P.W.M.N. van Leeuwen, *Homogeneous Catalysis: Understanding the Art*, Kluwer Academic Publishers, Dordrecht, 2004.
- [2] H.J. van der Westhuizen, R. Meijboom, A. Roodt, M. Schutte, *Inorg. Chem.* 49 (2010) 9599.
- [3] A. Roodt, H.G. Visser, A. Brink, *Crystallogr. Rev.* 17 (2011) 241.
- [4] M. Schutte, G. Kemp, H.G. Visser, A. Roodt, *Inorg. Chem.* 50 (2011) 12486.
- [5] A. Brink, H.G. Visser, A. Roodt, *Polyhedron* (2012), <http://dx.doi.org/10.1016/j.poly.2012.08.059>.
- [6] R. Crous, M. Datt, D. Foster, L. Bennie, C. Steenkamp, J. Huyser, L. Kirsten, G. Steyl, A. Roodt, *Dalton Trans.* (2005) 1108.
- [7] S. Otto, A. Roodt, *Inorg. Chim. Acta.* 357 (2004) 1.
- [8] A. Roodt, S. Otto, G. Steyl, *Coord. Chem. Rev.* 245 (2003) 125.
- [9] C. Sacht, M.S. Datt, S. Otto, A. Roodt, *J. Chem. Soc., Dalton Trans.* (2000) 4579.
- [10] D.E. Graham, G.J. Lamprecht, I.M. Potgieter, A. Roodt, J.G. Leipoldt, *Transition Met. Chem.* 16 (1991) 193.
- [11] A. Brink, H.G. Visser, A. Roodt, G. Steyl, *Dalton Trans.* 39 (2010) 5572.
- [12] M.T. Johnson, R. Johansson, M.V. Kondrashov, G. Steyl, M.S.G. Ahlquist, A. Roodt, O.F. Wendt, *Organometallics* 29 (2010) 3521.
- [13] D.J. Bray, J.K. Clegg, L.F. Lindoy, D. Schilter, *Adv. Inorg. Chem.* 59 (2007) 1.
- [14] G. Aromí, P. Gamez, J. Reedijk, *Coord. Chem. Rev.* 252 (2008) 964.
- [15] T.N. Hill, A. Roodt, G. Steyl, *Acta Cryst. B*, accepted for publication.
- [16] S. Otto, *Structural and Reactivity Relationships in Platinum(II) and Rhodium(II) Complexes*, Ph.D. Thesis, University of the Free State, Bloemfontein, South Africa, 1999.
- [17] Bruker CCD, Oxford Diffraction Ltd., Abingdon, Oxfordshire, UK, 2005.
- [18] Bruker SAINT-PLUS (including XPREP), Version 7.12, Bruker AXS Inc., Madison, WI, 2004.
- [19] Bruker SADABS (Version 2004/1), Bruker ASX Inc., Madison, WI, 1998.
- [20] CrysAlis RED Oxford Diffraction Ltd, Abingdon, Oxfordshire, UK, 2005.
- [21] G.M. Sheldrick, *Acta Cryst. A* 64 (2008) 112.
- [22] L.J. Farrugia, *Appl. Cryst.* 32 (1999) 837.
- [23] A.L. Spek, PLATON A Multipurpose Crystallographic Tool, Utrecht University, Utrecht, Netherlands, 2005.
- [24] A.L. Spek, *J. Appl. Cryst.* 36 (2003) 7.
- [25] A.L. Spek, *Acta Cryst. D* 65 (2009) 148.
- [26] M. Nardelli, *J. Appl. Cryst.* 28 (1995) 659.
- [27] K. Brandenburg, M. Brendt, DIAMOND, Release 2.1e, Crystal Impact GbR, Potfach 1251, D53002 Bonn, Germany, 2001.
- [28] HyperChem™ Release 7.52, Windows Molecular Modeling System, HyperCube Inc., 2002.
- [29] M.J. Frisch, G.W. Trucks, H.B. Schlegel, G.E. Scuseria, M.A. Robb, J.R. Cheeseman, J.A. Montgomery Jr., T. Vreven, K.N. Kudin, J.C. Burant, J.M. Millam, S.S. Iyengar, J. Tomasi, V. Barone, B. Mennucci, M. Cossi, G. Scalmani, N. Rega, G.A. Petersson, H. Nakatsuji, M. Hada, M. Ehara, K. Toyota, R. Fukuda, J. Hasegawa, M. Ishida, T. Nakajima, Y. Honda, O. Kitao, H. Nakai, M. Klene, X. Li, J.E. Knox, H.P. Hratchian, J.B. Cross, V. Bakken, C. Adamo, J. Jaramillo, R. Gomperts, R.E. Stratmann, O. Yazyev, A.J. Austin, R. Cammi, C. Pomelli, J.W. Ochterski, P.Y. Ayala, K. Morokuma, G.A. Voth, P. Salvador, J.J. Dannenberg, V.G. Zakrzewski, S. Dapprich, A.D. Daniels, M.C. Strain, O. Farkas, D.K. Malick, A.D. Rabuck, K. Raghavachari, J.B. Foresman, J.V. Ortiz, Q. Cui, A.G. Baboul, S. Clifford, J. Cioslowski, B.B. Stefanov, G. Liu, A. Liashenko, P. Piskorz, I. Komaromi, R.L. Martin, D.J. Fox, T. Keith, M.A. Al-Laham, C.Y. Peng, A. Nanayakkara, M. Challacombe, P.M.W. Gill, B. Johnson, W. Chen, M.W. Wong, C. Gonzalez, J.A. Pople, GAUSSIAN Inc., Wallingford, CT, 2004.
- [30] A.D. Becke, *J. Chem. Phys.* 98 (1993) 5648.
- [31] C. Lee, W. Yang, R.G. Parr, *Phys. Rev. B* 37 (1988) 785.
- [32] R. Ditchfield, W.J. Hehre, J.A. Pople, *J. Chem. Phys.* 54 (1971) 724.
- [33] M.S. Gordon, *Chem. Phys. Lett.* 76 (1980) 163.
- [34] V.A. Rassolov, M.A. Ratner, J.A. Pople, P.C. Redfern, L.A. Curiss, *J. Comp. Chem.* 22 (2001) 976.
- [35] P.J. Hay, W.R. Wadt, *J. Chem. Phys.* 82 (1985) 299.
- [36] A.P. Scott, L. Radom, *J. Phys. Chem.* 100 (1996) 16502.
- [37] M. Mikami, I. Nakagawa, T. Shimanouchi, *Spectrochim. Acta* A23 (1967) 1037.
- [38] N. Nakamoto, P.J. McCarthy, A. Ruby, A.E. Martell, *J. Am. Chem. Soc.* 83 (1066) (1961) 1272.
- [39] (a) K. Venkatasubramanian, *Indian J. Phys.* A56 (1982) 201;
(b) K. Venkatasubramanian, *Proc. Indian Acad. Sci., Chem. Sci.* 93 (1984) 1237.